AIAA JOURNAL
Vol. 43, No. 12, December 2005

Approximate Solution for the Compression Buckling of Fully Anisotropic Cylindrical Shells

Kian Foh Wilson Wong* and Paul M. Weaver†
University of Bristol, Bristol BS8 1TR, United Kingdom

The circular cylindrical thin-walled shell is a fundamental building block of many structures, such as aircraft fuselages. When used with laminated composites, highly efficient structures can be designed. As a result, the analytical treatment of cylindrical shells has received significant attention over recent decades. However, most of the works carried out in this area concern isotropic materials or orthotropic laminates, that is, those with no couplings. The present analysis develops a closed-form, yet simple solution for the linear buckling of laminated circular cylindrical shell, from the Donnell's model, including all available couplings. Although the usefulness of a linear solution for predicting buckling loads is questionable, its worth is in initial sizing and layup selection during the early stages of design. The resulting model could be used to examine the usefulness of different couplings that are not yet well understood. It is found that extension/shear coupling results in torsional movement of the cylinder, which, when restricted, induces a secondary torsional loading on the cylinder, thus reducing its overall buckling load by up to 50%. When not restricted, extension/shear couplings generally increase buckling loads.

Nomenclature

$[A_{ij}]$	=	in-plane stiffness
$[a_{ij}]$	=	$[A]^{-1}$ membrane compliance
$[B_{ij}]$	=	extension/flexural coupling
$[b_{ij}]$	=	$[A]^{-1}[B]$ eccentricity matrix
$[D_{ij}]$	=	flexural stiffness
$[d^*_{ij}]$	=	$[D]-[B][A]^{-1}[B]$ modified bending stiffness
F, W	=	maximum amplitude
l	=	length of cylinder
M_x, M_y, M_{xy}	=	moment resultants per unit length
m'	=	slope of spiral
N_x, N_y, N_{xy}	=	in-plane force resultants per unit length
n	=	number of circumferential waves
P	=	external axial compression per unit length
p	=	number of overall longitudinal waves
Q_x, Q_y	=	out-of-plane force resultants
r	=	radius of cylinder
t	=	thickness of laminate
u	=	axial displacement
v	=	circumferential displacement
w	=	radial displacement
x	=	axial coordinate
y	=	circumferential coordinate
z	=	radial coordinate
γ_A, δ_A	=	extension-shear anisotropy factors
γ_D, δ_D	=	flexural-twist anisotropy factors
γ_{xy}	=	in-plane shear strain resultant
$\varepsilon_x, \varepsilon_y$	=	in-plane direct strain resultants
$\kappa_x, \kappa_y, \kappa_{xy}$	=	out-of-plane curvatures
λ_m	=	axial wavelength
λ_n	=	circumferential wavelength
Φ	=	Airy's stress function

Presented as Paper 2004-2052 at the AIAA/ASME/ASCE/AHS/ASC 45th Structures, Structural Dynamics, and Materials Conference, AIAA/ASME/AHS 12th Adaptive Structures Conference, AIAA 6th Non-Deterministic Approaches Forum, and AIAA 5th Gossamer Spacecraft Forum, Palm Springs, CA, 19–22 April 2004; received 17 May 2004; revision received 31 May 2005; accepted for publication 2 June 2005. Copyright © 2005 by Kian Foh Wilson Wong and Paul M. Weaver. Published by the American Institute of Aeronautics and Astronautics, Inc., with permission. Copies of this paper may be made for personal or internal use, on condition that the copier pay the $10.00 per-copy fee to the Copyright Clearance Center, Inc., 222 Rosewood Drive, Danvers, MA 01923; include the code 0001-1452/05 $10.00 in correspondence with the CCC.

*Graduate Student, Department of Aerospace Engineering, Queen's Building, University Walk; Wilson.Wong@bristol.ac.uk. Student Member AIAA.

†Reader, Department of Aerospace Engineering, Queen's Building, University Walk; Paul.Weaver@bristol.ac.uk. Member AIAA.

Introduction

THE attractive properties of laminated composite materials have generated much interest in the pursuit of the understanding of their fundamental structural behavior. This is especially true in modern, high-performance applications where structures with high strength and stiffness to weight ratios are required. A fundamental component of many lightweight structures, such as aircraft and spacecraft, is the circular cylindrical shell. One particular area of interest is its buckling strength under compression loads.

In the past few decades, numerous publications[1–9] have appeared on the buckling analysis of anisotropic materials because of the increasing usage of laminated anisotropic materials in the aerospace industry. The anisotropic shell theories[1,2,10,11] used in these analyses are mostly extensions of the various isotropic shell models.[12–17] However, most of these models (which are cited in Ref. 6) have been limited to symmetric laminates in their usage in buckling analysis, without anisotropic couplings responses. This is partly because of the increased complexity when these couplings are introduced. This in turn precludes many benefits of laminated material, particularly the ability to tailor the material to the required properties.

Of course, there are also authors who included the different couplings in their models.[1–8] Of particular merit are the works of Cheng and Ho[1] and Khot and Venkayya.[2] The former developed closed-form, yet cumbersome expressions, based on the Flugge shell theory, whereas the latter, used Donnell's equations to develop expressions that are a generalization of the expressions derived in the current paper for shells of finite length. Little work appears to focus on the effects of the various forms of anisotropy on design. Recently, Weaver[7,8] gave a closed-form solution incorporating the flexural/twist and extension/twist anisotropy in its derivation, and as such builds on the classical orthotropic expressions given, for example, by Vasiliev,[18] which are based on Donnell's shell equations. The present work extends it further by including the extension-shear and extension-flexural couplings into the analysis. This work was carried out without prior knowledge of Khot and Venkayya's[2] achievements. However, the current work develops a closed-form solution that is simpler and is easier to use in subsequent layup and sizing optimization studies and fits into current ideas on buckling calculations for design[19] by providing a solution for the first level of design.

Although small geometric imperfections are well known to greatly diminish the buckling loads for isotropic cylindrical shells, there is mounting evidence that the effect is less in composites. In the experiments that were done by Hilburger and Starnes[20] and Meyer-Piening et al.,[21] it was shown that the knockdowns in buckling load as a result of geometric imperfections in orthotropic shells were generally lower (average of about 20%, depending on the stacking sequences used) than that in the isotropic shells (about 50%). As such, there remains a need and motivation to characterise the linear buckling behavior of composite shells.

It is the purpose of the present work to accomplish the task of taking full account of all of the couplings and yet give a simple and elegant closed-form solution to the problem of cylindrical shell buckling. In particular, we assess the effect of extension/shear coupling on buckling loads for a certain class of quasi-isotropic layup. It is hoped that the resulting formulas can prove useful in initial sizing and layup studies.

Derivation of Model

The shell model is based on Donnell's formulation, whereby the variation of twisting moment is neglected in the in-plane equilibrium equations. The reason for choosing Donnell's model is that it is applicable to a wide range of structural problems and yet simple and easy to manipulate. This allowed the complexity of the derivation to be reduced to a minimum as a first step in considering full anisotropic couplings in a laminate.

In solving the buckling problem of a circular cylindrical shell, a different approach was used from Donnell. Here, the authors used the semi-inverted constitutive equations to solve the problem, as first proposed by Stavsky and Hoff[22] and similar to the approach adopted by Geier et al.[6] The constitutive law can be written as

$$\{\varepsilon\} = [a]\{N\} - [b]\{\kappa\} \tag{1a}$$

$$\{M\} = [b]^T\{N\} + [d^*]\{\kappa\} \tag{1b}$$

The information needed now is the expressions for $\{N\}$ and $\{\kappa\}$, whereas all of the coefficient matrices can be found from the stiffness of the laminate considered. Donnell's expressions for the out-of-plane curvatures are

$$\kappa_x = -\frac{\partial^2 w}{\partial x^2}, \qquad \kappa_y = -\frac{\partial^2 w}{\partial y^2}, \qquad \kappa_{xy} = -2\frac{\partial^2 w}{\partial x \partial y} \tag{2}$$

with the coordinate system shown in Fig. 1. For the expression of the in-plane force resultant, the Airy's stress function Φ is employed, as in the case of two-dimensional elasticity. Thus, the force resultant can be represented as follows:

$$N_x = \frac{\partial^2 \Phi}{\partial y^2}, \qquad N_y = \frac{\partial^2 \Phi}{\partial x^2}, \qquad N_{xy} = -\frac{\partial^2 \Phi}{\partial x \partial y} \tag{3}$$

The equilibrium equations given by Donnell are

$$\frac{\partial N_x}{\partial x} + \frac{\partial N_{xy}}{\partial y} = 0 \tag{4a}$$

$$\frac{\partial N_y}{\partial y} + \frac{\partial N_{xy}}{\partial x} = 0 \tag{4b}$$

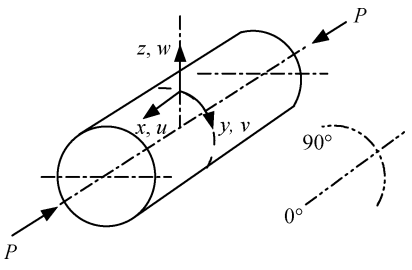

Fig. 1 Coordinate system.

$$\frac{\partial Q_x}{\partial x} + \frac{\partial Q_y}{\partial y} - \frac{N_y}{r} - P\frac{\partial^2 w}{\partial x^2} = 0 \tag{4c}$$

$$\frac{\partial M_x}{\partial x} + \frac{\partial M_{xy}}{\partial y} = Q_x \tag{4d}$$

$$\frac{\partial M_y}{\partial y} + \frac{\partial M_{xy}}{\partial x} = Q_y \tag{4e}$$

The use of the Airy's stress function results in the first two equations (4a) and (4b) being satisfied automatically. Therefore, the only equations remaining are Eqs. (4c–4e). They are not independent as Eqs. (4d) and (4e) can be differentiated once and when substituted into Eq. (4c), one can obtain the following governing equation:

$$\frac{\partial^2 M_x}{\partial x^2} + 2\frac{\partial^2 M_{xy}}{\partial x \partial y} + \frac{\partial^2 M_y}{\partial y^2} - \frac{N_y}{r} - P\frac{\partial^2 w}{\partial x^2} = 0 \tag{5}$$

To solve the problem at hand, another expression is needed, and this can be found from the compatibility condition of the strains. The strains for the Donnell's model can be written as

$$\varepsilon_x = \frac{\partial u}{\partial x}, \qquad \varepsilon_y = \frac{\partial v}{\partial y} + \frac{w}{r}, \qquad \gamma_{xy} = \frac{\partial u}{\partial y} + \frac{\partial v}{\partial x} \tag{6}$$

which must satisfy the compatibility condition

$$\frac{\partial^2 \varepsilon_x}{\partial y^2} + \frac{\partial^2 \varepsilon_y}{\partial x^2} - \frac{\partial^2 \gamma_{xy}}{\partial x \partial y} = \frac{1}{r}\frac{\partial^2 w}{\partial x^2} \tag{7}$$

By substituting Eqs. (2) and (3) into Eq. (1) and then into the two governing equations (5) and (7), one obtains

$$\begin{aligned} &a_{22}\frac{\partial^4 \Phi}{\partial x^4} - 2a_{26}\frac{\partial^4 \Phi}{\partial x^3 \partial y} + (2a_{12} + a_{66})\frac{\partial^4 \Phi}{\partial x^2 \partial y^2} \\ &\quad -2a_{16}\frac{\partial^4 \Phi}{\partial x \partial y^3} + a_{11}\frac{\partial^4 \Phi}{\partial y^4} - \frac{1}{r}\frac{\partial^2 w}{\partial x^2} \\ &\quad + \left[b_{21}\frac{\partial^4 w}{\partial x^4} - (b_{61} - 2b_{26})\frac{\partial^4 w}{\partial x^3 \partial y} + (b_{11} + b_{22} - 2b_{66})\frac{\partial^4 w}{\partial x^2 \partial y^2} \right. \\ &\quad \left. - (b_{62} - 2b_{16})\frac{\partial^4 w}{\partial x \partial y^3} + b_{12}\frac{\partial^4 w}{\partial y^4} \right] = 0 \end{aligned} \tag{8a}$$

$$\begin{aligned} &d_{11}^*\frac{\partial^4 w}{\partial x^4} + 4d_{16}^*\frac{\partial^4 w}{\partial x^3 \partial y} + 2\left(d_{12}^* + 2d_{66}^*\right)\frac{\partial^4 w}{\partial x^2 \partial y^2} + 4d_{26}^*\frac{\partial^4 w}{\partial x \partial y^3} \\ &\quad + d_{22}^*\frac{\partial^4 w}{\partial y^4} - \left[b_{21}\frac{\partial^4 \Phi}{\partial x^4} - (b_{61} - 2b_{26})\frac{\partial^4 \Phi}{\partial x^3 \partial y} \right. \\ &\quad + (b_{11} + b_{22} - 2b_{66})\frac{\partial^4 \Phi}{\partial x^2 \partial y^2} - (b_{62} - 2b_{16})\frac{\partial^4 \Phi}{\partial x \partial y^3} \\ &\quad \left. + b_{12}\frac{\partial^4 \Phi}{\partial y^4} \right] + \frac{1}{r}\frac{\partial^2 \Phi}{\partial x^2} + P\frac{\partial^2 w}{\partial x^2} = 0 \end{aligned} \tag{8b}$$

To solve these two equations, a trial solution for the radial displacement and the Airy's stress function needs to be established and is suggested as

$$w = W\sin(\lambda_n y - \lambda_m x), \qquad \Phi = F\sin(\lambda_n y - \lambda_m x) \tag{9}$$

The definition of the circumferential wavelength λ_n remains the same as that in classical theory, whereas the axial wavelength λ_m has the definition as found by Weaver[7,8]:

$$\lambda_m = m'n/r, \qquad \lambda_n = n/r \tag{10}$$

Note that the presence of angle-ply anisotropy ensures that the favorable buckling mode is skew in nature and reminiscent of a torsional

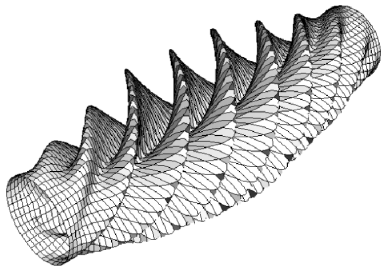

Fig. 2 Spiral mode in anisotropic shell compression buckling.

buckling mode. As such, the term m' is the gradient of the spiral as measured by a line of constant radial amplitude. It can be defined as the ratio of circumferential to longitudinal travel for the spiral. Therefore, it is not the normal discrete number of longitudinal half-waves, but a continuous variable that can be either positively or negatively valued.

These basis functions do not satisfy the boundary condition of the shell and as such are approximate in nature. Since this work was conducted, it has come to the attention of the authors that Khot and Venkayya[2] carried out similar work. Their displacement function was

$$w = W \sin(p\pi x/l) \sin(\lambda_n y - \lambda_m x) \tag{11}$$

from which the stress function Φ was deduced from the compatibility equation. It appears they did not realize that the first sine term in the expression for w generally always has $p = 1$. Its value represents an overall sine wave superposed on top of the spirally induced deformation of the second sine term. Its presence ensures zero displacement but notably, not the zero bending moment at the ends of the shell. A buckling mode with $p = 1$ is shown in Fig. 2. If p and n values were continuous and not integer in nature, then p would always equal unity. However, on occasion a greater value of p can be obtained, as a direct result of variable discretization, to give marginally lower buckling loads. This does not occur for medium length shells for which $m'n/(rl) \ll 1$, then the current solution for buckling load is indistinguishable from that of Khot and Venkayya, and yet is fundamentally simpler because one of the variables p has been eliminated. Furthermore, the shell needs to be of sufficient length that the Batdorf parameter $l^2/(rt)$ is not small, typically greater than 100, and that the length parameter l^2t/r^3 is less than 3 (Ref. 7).

The trial displacement equations (9) can then be substituted into Eq. (8), where the trigonometric terms cancel. A coefficient matrix could be obtained by grouping the two equations into matrix form with W and F as variables. Following the approach used in Cheng and Ho,[1] the determinant of the coefficient matrix must equal zero in order to have a valid solution. After reformulating for P, one obtains the following closed-form solution for the buckling load of a laminated circular cylindrical shell under compression:

$$P = \frac{1}{\lambda_m^2}\begin{bmatrix} d_{11}^*\lambda_m^4 - 4d_{16}^*\lambda_m^3\lambda_n + 2\left(d_{12}^* + 2d_{66}^*\right)\lambda_m^2\lambda_n^2 \\ -4d_{26}^*\lambda_m\lambda_n^3 + d_{22}^*\lambda_n^4 \end{bmatrix} + \frac{\begin{bmatrix} b_{21}\lambda_m^4 + (b_{61} - 2b_{26})\lambda_m^3\lambda_n + (b_{11} + b_{22} - 2b_{66})\lambda_m^2\lambda_n^2 \\ +(b_{62} - 2b_{16})\lambda_m\lambda_n^3 + b_{12}\lambda_n^4 + \lambda_m^2/r \end{bmatrix}^2}{\lambda_m^2\left[a_{22}\lambda_m^4 + 2a_{26}\lambda_m^3\lambda_n + (2a_{12} + a_{66})\lambda_m^2\lambda_n^2 + 2a_{16}\lambda_m\lambda_n^3 + a_{11}\lambda_n^4\right]} \tag{12}$$

The buckling load is found by iterating through different values of m' and n to obtain the lowest possible value of P. This is because the structure will lose stability with the lowest energy possible, which corresponds to one particular mode shape, described by m' and n. The first part of Eq. (12) is comparable to the buckling equation for a plate. The second part can be further seen as a combination of the extension/flexural couplings terms (those with $[b]$ elements as coefficients) and the membrane terms.

Table 1 Material properties of T800-924 (CFRP) prepreg

Property	Value
E_{11}, GPa	161.000
E_{22}, GPa	11.500
G_{13}, GPa	7.169
ν_{12}	0.349

Validation of Results by Finite Element Analysis

The results obtained from finite element analysis (FEA) were taken as the reference for which the results calculated from Eq. (12) will be compared. The FEA allows a model without any imperfection but with the necessary end conditions to simulate real structural boundary conditions, thus giving an idea of the usefulness of the analytical model in more realistic circumstances. ABAQUS/Standard Solver was chosen as the FEA platform, and the eigenvalue buckling analysis of the Standard Solver gave the linear buckling load of the model. The material used in the analysis was the T800-924 carbon-fiber-reinforced plastic prepreg, with its properties shown in Table 1.

The circular cylinder modeled has the following dimensions: radius, 80 mm; length, 150 mm; and ply thickness, 0.125 mm. These are chosen to avoid any interaction between local buckling and Euler buckling. The mesh has 45 elements longitudinally and 80 elements circumferentially, where the parabolic thick shell element S8R was used and the aspect ratio of the elements were kept below two. At both ends of the cylinder, rigid elements R3D3 were connected to the S8R shell elements around the circumference, constraining the ends to stay circular and not allowing any deformation. These rigid elements have the centers at both ends of the cylinder as their reference points. The support was fully fixed allowing axial displacement and rotation about the x axis at one end (SS4). The mesh was refined and tested against its convergence, where its eigenvalue results and buckling mode shapes were compared with that of the analytical solution. The whole length of the cylinder was modeled and as such did not employ any limiting symmetry conditions, as is required because of the asymmetric spiral mode shape.[7]

The layups analyzed were chosen based on the couplings that were present, with their orientations given in the Appendix. The results from both the analytical prediction and FEA were shown in Table 2. It is shown that the prediction is within 2% of the FEA, which is similar to the accuracy as found in Weaver[7] and is not surprising because the present model is an extension. The analytical solutions found for layups with either extension-twist or bend-twist couplings only were also compared with those found previously[8] and were found to agree exactly. The model is thus validated, against both the FEA and an earlier analytical model.[8]

Further Analysis: Finite Element Analysis

The FEA was repeated with the same group of layups, but now with fully fixed support allowing only axial displacement at one end (SS3). The results are also presented in Table 2. It was found that the discrepancy between the two different types of boundary conditions could be as large as 5% for some of the layups. Those layups that are found to have significant discrepancy are those with the presence of the extension-shear couplings. This suggests that extension-shear couplings are the source of the discrepancy.

Further investigation into the reaction forces using results generated from the static analysis of ABAQUS revealed the presence of a secondary induced load in the structure, which is torsional in nature. In the investigation, it was found that laminates with either extension-twist or bend-twist couplings also induce torsion in the structure but without any significant effect to the buckling load. Upon close scrutiny of the internal forces from the FEA, the induced torsion originates from the internal shear forces and internal twisting moment at the edge. The internal shear forces were found to be the dominant contribution towards the resultant torsional load. The torsion caused by the internal twisting moment, generated by the extension-twist or bend-twist couplings, is small when compared to

Table 2 Buckling load results N calculated using the analytical model, FFA employing SS3 and SS4, and their relative errors

Layup	FEA/SS4	FEA/SS3	Present model[a]	Error, %[b]	Error, %[c]	Couplings present
i	156,319	156,317	158,000	1.1	0.0	D_{16}, D_{26}
ii	169,105	169,239	172,000	1.7	0.0	B_{16}, B_{26}
iii	137,803	130,388	138,000	0.1	−5.4	A_{16}, A_{26}, D_{16}, D_{26}
iv	28,729	28,729	28,700	−0.1	0.0	B_{11}, B_{22}
v	156,049	156,049	158,000	1.3	0.0	B_{11}, B_{22}, B_{12}, B_{66}
vi	193,666	194,374	196,000	1.2	0.4	B_{11}, B_{22}, B_{16}, B_{26}
vii	186,013	186,415	190,000	2.1	0.2	Full B matrix
viii	168,308	175,600	170,000	1.0	4.3	A_{16}, A_{26}, B_{16}, B_{26}, D_{16}, D_{26}
ix	152,581	160,071	154,000	0.9	4.9	All couplings included

[a]Results correct to three significant figures. [b]Comparison of analytical prediction with FEA/SS4. [c]Comparison of results from FEA/SS3 with FEA/SS4.

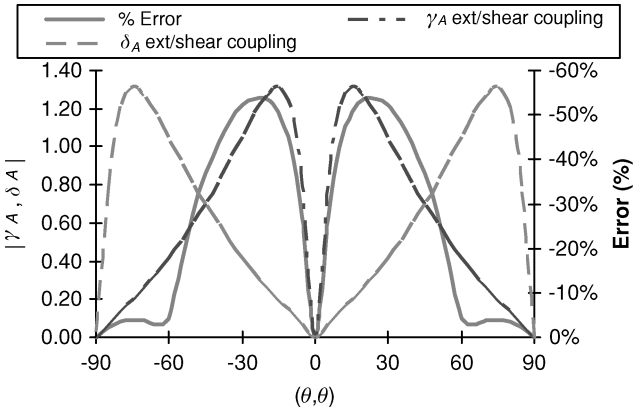

Fig. 3 Variation of the FEA results discrepancies corresponding to variation of extension-shear anisotropy.

the compression loading; thus, its effect is deemed negligible within this linear analysis. However, its presence can have significance within a nonlinear postbuckling model. From FE-based empirical studies, using laminates with different couplings tested in FEA, the effect of the induced secondary torsion becomes significant when the percentage of the torsional stress of the induced torsional moment to the compression stress of the loading is greater than unity, which happens when extension-shear couplings are present. Thus, it is concluded that the extension-shear coupling induces a secondary torsional loading on a rotationally restrained cylinder, resulting in a combined state of compression and torsional loading, which in turn reduces the buckling load of the cylinder.

The amount of reduction of the buckling load depends on the magnitude of the extension-shear coupling. A parametric study was done using FEA on single-layer symmetric laminates θ, as this gives the maximum and minimum range of extension-shear couplings for a specific material, and also eliminates the effects of $[B]$ couplings that would otherwise affect buckling loads. The magnitudes of the extension-shear couplings are quantified by the anisotropy factors introduced by Nemeth[23]:

$$\gamma_A = -a_{16} \Big/ \sqrt[4]{a_{11}^3 a_{22}}, \qquad \delta_A = -a_{26} \Big/ \sqrt[4]{a_{11} a_{22}^3} \tag{13}$$

The parametric study examined the discrepancy of the FEA results between SS3 and SS4 support conditions and their relation with the amount of extension-shear anisotropy. Figure 3 shows the results of the parametric study, where the error represents the deviation of the buckling load for SS3 from SS4.

From Fig. 3, it is clear that the discrepancy is strongly correlated with γ_A, where the error curve follows almost exactly the path of γ_A. Detailed observation of the figure reveals that δ_A also contributes to the error term. From angles of ± 60 to ± 90 deg, where δ_A dominates, the diminishing error curve experiences a small local maxima before reducing to zero. This is intuitively understandable if one thinks of the physical meaning of A_{16}, which is the main shear coupling when axial compression is applied, and A_{26}, which is the Poisson's effect shear coupling in this case. This phenomenon can also be explained analytically by looking at the constitutive equation in the compliance matrix form. For a two-layer symmetric laminate, the $[B]$ matrix is zero. The only applied loading is the compression load N_x. The third row of Eq. (14) shows that this compression load will result in in-plane shearing deformation of an element, with a_{16} as the direct magnification factor. For SS3, where this shearing deformation is restrained, it is reacted by a torsional load at the ends of the cylinder. As such, this explanation justifies γ_A as the main contributing factor to the discrepancy between SS3 and SS4 boundary conditions:

$$\begin{Bmatrix} \varepsilon_x \\ \varepsilon_y \\ \gamma_{xy} \end{Bmatrix} = \begin{bmatrix} a_{11} & a_{12} & a_{16} \\ a_{12} & a_{22} & a_{26} \\ a_{16} & a_{26} & a_{66} \end{bmatrix} \begin{Bmatrix} N_x \\ N_y \\ N_{xy} \end{Bmatrix} \tag{14}$$

Upon examination of the second row of Eq. (14), one observes that N_x causes a circumferential deformation through a_{12}. As this is restricted by SS3, it reacts as internal N_y in the element, which also act through a_{26} to give a resultant torsional load, albeit to a much smaller magnitude. Therefore, local maximum is observed at the trailing ends of the error curve in Fig. 3, which is caused by δ_A. The overall induced shear at buckling can be approximated by

$$N_{xy} = -(a_{16}/a_{66})N_x \tag{15}$$

where N_x in Eq. (15) refers to the reduced buckling load with boundary condition SS4, not the buckling load with boundary condition SS3.

The importance of this study is to show that the discrepancy can be significant, up to 50% for cases shown here, which means the buckling load with SS3 is only half that of SS4. Furthermore, the range 5 deg $\leq |\theta| \leq$ 50 deg gives errors in the range (25–55%), which has implications on design if manufacturing tolerances on fiber angle for 0-deg fibers are significant.

The conclusion from this particular error analysis is that when a compressive load is applied to a laminated cylinder with extension-shear couplings and with boundary condition SS3 the cylinder is actually experiencing a combined loading of compression and torsion, which reduces its buckling load considerably from that predicted by just the compressive load, depending on the magnitude of the extension-shear couplings. Thus one has to be careful when designing such a structure to take into account this secondary induced load.

If extension-shear couplings are inevitable, it would be advised that one should design towards larger a_{26} as it leads to a smaller induced load. However, this only applies if the laminate has unequal γ_A and δ_A. Preferential fiber angles to use would be $|\theta| > 50$ deg. These angles would of course results in lower longitudinal strength, and thus a tradeoff has to be made between reduction in buckling load and longitudinal strength.

On the other hand, one could make use of this knowledge to increase the buckling load of a structure undergoing both compression and torsion loadings, by designing for a laminate with an induced torsion opposite to the direction to the applied torsion. This would have to be done by iterating through the design with results from

FEA, as there is not yet an analytical solution to accurately calculate the induced torsion caused by the extension-shear couplings.

Further Analysis: Analytical

Another parametric study was done using the analytical model to investigate the effect of extension-shear couplings on the buckling load. It should be apparent from the last section that the analytical model is a representation of the FEA model for the situation where the rotation about the x axis is allowed (SS4). Thus there is no reduction in the buckling load caused by the secondary induced torsional load.

The layups are all quasi-isotropic in nature (with equal numbers of 0-, 90-, 45-, and −45-deg ply angles). They are also homogeneous in the sense that

$$D_{ij}/A_{ij} = t^2/12 \qquad \text{for} \qquad i, j \neq 6$$

is satisfied, yet have different amounts of membrane and flexural anisotropy. They are listed in the Appendix and are taken from Ref. 8. To obtain layups with extension-shear couplings from these current 48 layers layups, they have to be modified accordingly. Instead of the number of ±45 deg being equal, they are made unequal but keeping the fact that the total sum of ±45 deg should still be the same. This would allow a large combination of layups with extension-shear couplings from these basic sets. It is impossible to obtain a homogeneous, quasi-isotropic layup with only extension-shear couplings and no other couplings in 48 layers, as the bend-twist couplings will always be present. Therefore, the bend-twist couplings need to be quantified properly as well. This is done in the same way as has been described by Weaver,[7] where the anisotropy factors introduced by Nemeth[23]

$$\gamma_D = D_{16} \Big/ \sqrt[4]{D_{11}^3 D_{22}}, \qquad \delta_D = D_{26} \Big/ \sqrt[4]{D_{11} D_{22}^3} \qquad (16)$$

are again used. Using these anisotropy factors, and those introduced in Eq. (13), the effect of extension-shear couplings can then be studied. The results of the parametric study are shown in Fig. 4. For the particular class of laminates studied here, the two bend-twist anisotropy factors are always equal to each other. The knockdown factor k_l is the knockdown in the buckling load compared to the quasi-isotropic layup ($E_{\text{iso}} = 63.4$ GPa, $\nu_{\text{iso}} = 0.3$).

As shown in Fig. 4, for the case where there are no extension-shear couplings, the knockdown caused by bend-twist anisotropy factors is as expected according to Ref. 7. The line with $\gamma_D, \delta_D = 0$ is calculated analytically; as has already been mentioned, there are no laminates with only extension-shear couplings in 48 layers involving the same degree of symmetry using the same ply orientations. For the case where bend-twist couplings exist, the extension-shear couplings can either increase or decrease the buckling load accordingly.

Generally, when the bend-twist couplings are positive, then positive (negative) extension-shear couplings will increase (decrease) the buckling load and vice versa. However, there seems to be a limit for increasing the buckling load. The relationship between γ_D, δ_D,

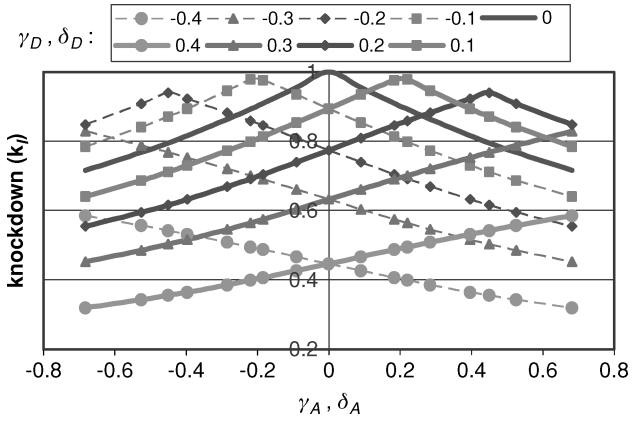

Fig. 4 Effect of extension-shear coupling on the classical buckling analysis.

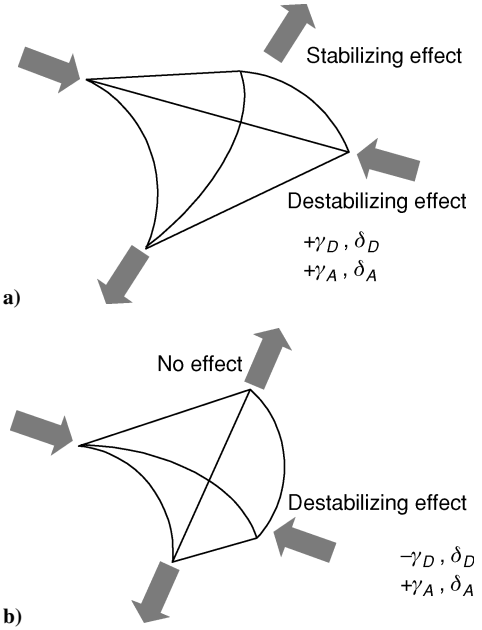

Fig. 5 Physical interpretation of extension-shear anisotropy effect with SS4 boundary condition.

and γ_A, δ_A to obtain the maximum buckling load can be described by a quadratic function, where its coefficients depend on the material used in the laminates. This can be closely approximated by a linear relation $(\gamma_D, \delta_D) = 2 \times (\gamma_A, \delta_A)$, with a goodness of fit of 0.993. Therefore, the following rules are applicable during the design stage:

For $+\gamma_D, \delta_D$, $+\gamma_A, \delta_A$ will increase the buckling load up until $2 \times \gamma_D, \delta_D$; and $-\gamma_A, \delta_A$ will decrease the buckling load.

For $-\gamma_D, \delta_D$, $-\gamma_A, \delta_A$ will increase the buckling load up until $2 \times \gamma_D, \delta_D$; and $+\gamma_A, \delta_A$ will decrease the buckling load.

The physical reasoning behind this effect is best shown graphically in Fig. 5. The figures show an edge element undergoing a twist deformation due to the presence of bend-twist couplings in the laminate. The direction of twist depends on the sign of the bend-twist couplings. A positive twisting is shown in Fig. 5a. The extension-shear couplings would induce shear forces at the edges of the element. However, in SS4 boundary condition the element is allowed to rotate around the x axis, and as such the shear is thus manifested as a displacement, which effectively is just tension and compression in the diagonals. The shear displacement, as a result of positive extension-shear anisotropy, is shown in Fig. 5. In the case of Fig. 5a, the diagonal where the tension acts is curved because of the positive twist; thus, the tension has a stabilizing effect on the twist as it tries to straighten the curved line (or flatten the element). This stabilizing effect reduces the deformation the element undergoes and thus increases the load-carrying capability of the element. The extent of this stabilization depends on the amount of twist present in the element. When tension exceeds the amount needed to undo the twist, the destabilizing effect starts to become significant, compressing the straight diagonal. This then reduces the buckling load as the absolute value of extension-shear couplings increase further.

In Fig. 5b, an element with negative bend-twist and positive extension-shear anisotropy is shown. Here, there is no stabilizing effect as the diagonal in tension is originally straight. However, the diagonal where the destabilizing effect acts is originally curved; thus, the compression will cause larger deformation. This reduces the load-carrying capacity of the element, and thus reduces the buckling load. Therefore, there is no bound in the reduction of the buckling load.

In conclusion, when there are bend-twist couplings in the laminates, one would design for extension-shear couplings according to the amount and sign of bend-twist couplings in order to increase the buckling load, with the reservation that this holds only in the SS4 boundary condition.

Conclusions

An approximate yet relatively simple closed-form solution for the linear buckling load of circular cylindrical shells has been developed from Donnell's model. It is shown to predict the buckling load to an accuracy of within 2% when compared with detail linear finite element analysis. It was found that the extension-shear couplings could induce a secondary torsional loading when the cylinder is restricted to rotate in the torsional sense, thus resulting in a combined compressive and torsional loading. This will reduce the buckling load of the cylinder considerably (up to 50%) depending on the magnitude of the extension-shear couplings. However, when the cylinder is free to rotate in the torsional sense, the extension-shear couplings could be tailored to increase the buckling load according to the amount and sign of the bend-twist couplings present. In conclusion, a designer should apply the following guidelines:

1) For cylinders with rotational restrictions, i.e., SS3, and with extension/shear coupling present, then one should design for laminates with larger a_{26} than a_{16} if they are not equal by using $|\theta| \geq 50$ deg.

2) For cylinder with rotational restriction (SS3), one can make use of the fact that extension/shear would induce secondary torsion to increase the buckling load of a cylinder undergoing both compression and torsion.

3) For cylinders without rotational restrictions, i.e., SS4, and with positive (negative) bend/twist anisotropy factors, then one should design to have positive (negative) extension/shear anisotropy factors (up to twice the bend/twist anisotropy factors), to increase the buckling load.

Finally, the current work has deliberately emphasized understanding of linear response before nonlinear postbuckling studies are attempted. Ignoring nonlinear effects can have adverse effects on practical design.

Appendix: Homogeneous Quasi-Isotropic Layups with Various Anisotropic Couplings

The orientation shown next has the bottom layer as the leftmost layer, while "s" represents symmetric layup and "as" represents the antisymmetric layup.

Layups used in Table 2 are given here:

i: (90, −45, 0, 45)s
ii: (90, −45, 0, 45)as
iii: (90, −45, −45, 0)s
iv: (90, 90, 90, 0)
v: (90, −45, 45, 45, 0, −45, −45, 45)
vi: (90, −45, 0, 45, −45, 90, 45, 0)
vii: (90, −45, 0, 45, 90, 0, −45, 45)
viii: (90, −45, 0, 45, −45, 0, −45, 90)
ix: (90, −45, 0, 45, 0, 0, 90, −45)

Layups used in further analysis/analytical are given here:

A (0, −45, 90, −45, 0, 45, 45, 90, −45, 90, 45, 45, 90, 0, 0, 90, 45, −45, 45, −45, 0, 0, 90, −45)s
B (0, −45, 90, −45, 0, −45, 45, 90, 45, 90, 45, 45, 90, 0, 0, 90, 45, −45, 45, −45, 0, 0, 90, −45)s
C (0, −45, 90, −45, 0, −45, −45, 90, 45, 90, 45, 45, 90, 0, 0, 90, 45, 45, 45, −45, 0, 0, 90, −45)s
D (0, −45, 90, −45, 0, −45, −45, 90, −45, 90, 45, 45, 90, 0, 0, 90, 45, 45, 45, 45, 0, 0, 90, −45)s
E (0, −45, 90, −45, 0, −45, −45, 90, −45, 90, −45, 45, 90, 0, 0, 90, 45, 45, 45, 45, 0, 0, 90, 45)s
F (0, −45, 90, 45, 0, −45, 45, 90, −45, 90, 45, −45, 90, 0, 0, 90, 45, −45, 45, 45, 0, 0, 90, −45)s
G (0, −45, 90, 45, 0, −45, −45, 90, 45, 90, −45, 45, 90, 0, 0, 90, 45, −45, 45, 45, 0, 0, 90, −45)s
H (0, −45, 90, 45, 0, −45, −45, 90, 45, 90, −45, 45, 90, 0, 0, 90, −45, −45, 45, 45, 0, 0, 90, 45)s
I (0, −45, 90, 45, 0, −45, −45, 90, 45, 90, −45, −45, 90, 0, 0, 90, 45, 45, 45, −45, 0, 0, 90, 45)s
J (0, −45, 90, −45, 0, −45, 45, 90, 45, 90, −45, −45, 90, 0, 0, 90, −45, 45, 45, 45, 0, 0, 90, 45)s
K (0, −45, 90, −45, 0, −45, −45, 90, 45, 90, −45, 45, 90, 0, 0, 90, −45, 45, 45, 45, 0, 0, 90, 45)s
L (−45, −45, −45, −45, 0, 90, 90, 90, 0, 0, 0, −45, 0, 90, 90, −45, 45, 45, 90, 45, 45, 0, 45, 45)s
M (−45, −45, −45, 0, −45, 90, 90, 90, 0, 0, 0, −45, −45, 90, 90, 45, 0, 0, 90, 45, 45, 45, 45, 45)s
N (−45, −45, −45, −45, 90, 90, 0, 0, 0, 0, 90, −45, 90, 0, −45, 90, 45, 90, 45, 45, 0, 45, 45, 45)s
O (−45, −45, −45, −45, 90, 90, 0, 0, 0, 90, −45, 90, 0, 0, 0, −45, 90, 45, 45, 45, 45, 90, 45, 45)s
P (−45, −45, −45, 90, −45, 0, 0, 0, −45, 90, 90, 90, 0, 90, −45, 90, 0, 0, 45, 45, 45, 45, 45, 45)s
Q (−45, 45, −45, 45, 0, 90, 90, 90, 0, 0, 0, −45, 0, 90, 90, −45, 45, −45, 90, 45, 45, 0, 45, −45)s
R (−45, −45, −45, 45, 0, 90, 90, 90, 0, 0, 0, 45, 0, 90, 90, −45, −45, 45, 90, 45, 45, 0, −45, 45)s
S (−45, −45, −45, 0, 45, 90, 90, 90, 0, 0, 0, 45, −45, 90, 90, 45, 0, 0, 90, 45, 45, −45, −45, 45)s
T (−45, −45, 45, 0, 45, 90, 90, 90, 0, 0, 0, 45, −45, 90, 90, −45, 0, 0, 90, −45, 45, 45, −45, 45)s
U (45, −45, −45, −45, 90, 90, 0, 0, 0, 0, 90, 45, 90, 0, −45, 90, 45, 90, −45, 45, 0, 45, −45, 45)s
V (−45, −45, −45, −45, 90, 90, 0, 0, 0, 0, 90, 45, 90, 0, 45, 90, −45, 90, 45, 45, 0, 45, 45, −45)s
W (−45, −45, −45, −45, 90, 90, 0, 0, 0, 90, 45, 90, 0, 0, 0, 45, 90, −45, 45, 45, −45, 90, 45, 45)s
X (45, −45, −45, −45, 90, 90, 0, 0, 0, 90, 45, 90, 0, 0, 0, −45, 90, 45, −45, −45, 45, 90, 45, 45)s
Y (−45, −45, −45, 45, 90, 90, 0, 0, 0, 90, −45, 90, 0, 0, 0, 45, 90, 45, −45, 45, 45, 90, −45, 45)s
Z (−45, −45, −45, −45, 90, 90, 0, 0, 0, 90, 45, 90, 0, 0, 0, 45, 90, 45, 45, 45, 45, 90, −45, −45)s
AA (−45, −45, −45, −45, 90, 90, 0, 0, 0, 90, 45, 90, 0, 0, 0, −45, 90, 45, −45, 45, 45, 90, 45, 45)s
AB (−45, −45, −45, −45, 90, 90, 0, 0, 0, 90, −45, 90, 0, 0, 0, 45, 90, 45, 45, 45, 45, 90, −45, 45)s
AC (−45, −45, −45, −45, 0, 90, 90, 90, 0, 0, 0, −45, 0, 90, 90, 45, 45, 45, 90, 45, 45, 0, 45, −45)s
AD (−45, −45, −45, 90, 45, 0, 0, 0, −45, 90, 90, 90, 0, 90, −45, 90, 0, 0, −45, 45, 45, 45, 45, 45)s

References

[1]Cheng, S., and Ho, B. P. C., "Stability of Heterogeneous Aeolotropic Cylindrical Shells Under Combined Loading," *AIAA Journal*, Vol. 1, No. 4, 1963, pp. 892–898.

[2]Khot, N. S., and Venkayya, V. B., "Effect of Fiber Orientation on Initial Postbuckling Behavior and Imperfection Sensitivity of Composite Cylindrical Shells," AFFL/TR/70/125, Wright–Patterson AFB, OH, June 1970.

[3]Fan, S. R., Geier, B., Rohwer, K., and Liu, D. C., "Stability of Layered Anisotropic Cylindrical Shells Under Combined Loading," *Zeitschrift für Flugwissenschaften und Weltraumforschung*, Vol. 7, No. 5, 1983, pp. 293–301.

[4]Bert, C. W., and Kim, C., "Analysis of Buckling of Hollow Laminated Composite Drive Shafts," *Composites Science and Technology*, Vol. 53, No. 3, 1995, pp. 343–351.

[5]Jaunky, N., and Knight, N. F., "An Assessment of Shell Theories for Buckling of Circular Cylindrical Laminated Composite Panels Loaded in Axial Compression," *International Journal of Solids and Structures*, Vol. 36, No. 25, 1999, pp. 3799–3820.

[6]Geier, B., Meyer-Piening, H.-R., and Zimmermann, R., "On the Influence of Laminate Stacking on Buckling of Composite Cylindrical Shells Subjected to Axial Compression," *Composites Structures*, Vol. 55, No. 4, 2002, pp. 467–474.

[7]Weaver, P. M., "Anisotropy-Induced Spiral Buckling in Compression-Loaded Cylindrical Shells," *AIAA Journal*, Vol. 40, No. 5, 2002, pp. 1001–1007.

[8]Weaver, P. M., "The Effect of Extension/Twist Anisotropy on Compression Buckling in Cylindrical Shells," *Composites Part B: Engineering*, Vol. 34, No. 3, 2003, pp. 251–260.

[9]Kapania, R. K., "A Review on The Analysis of Laminated Shells," *Journal of Pressure Vessel Technology*, Vol. 111, No. 2, 1989, pp. 88–96.

[10]Dong, S. B., Pister, K. S., and Taylor, R. L., "On the Theory of Laminated Anisotropic Shells and Plates," *Journal of the Aerospace Sciences*, Vol. 29, No. 8, 1962, pp. 969–975.

[11]Bert, C. W., "Structural Theory for Laminated Anisotropic Elastic Shells," *Journal of Composite Materials*, Vol. 1, No. 4, 1967, pp. 414–423.

[12]Love, A. E. H., *A Treatise on the Mathematical Theory of Elasticity*, 4th ed., Cambridge Univ. Press, Cambridge, England, U.K., 1927.

[13]Donnell, L. H., "Stability of Thin-Walled Tube Under Torsion," NACA Rept. 479, 1935, pp. 95–116.

[14]Flügge, W., *Stresses in Shells*, 2nd ed., Springer-Verlag, New York, 1973; *Statik und Dynamik der Schalen*, Springer-Verlag, Berlin, 1934.

[15]Sanders, J. L., "An Improved First-Approximation Theory for Thin Shells," NASA TR/R/24, 1959.

[16]Koiter, W. T., "A Consistent First Approximation in the General Theory of Thin Elastic Shells," *Proceedings of the Symposium on Theory of Thin Elastic Shells*, edited by W. T. Koiter, North-Holland, Delft, The Netherlands, 1960, pp. 12–33.

[17]Vlasov, V. Z., "General Theory of Shells and Its Applications in Engineering," NASA TT F/99, 1964; also "Obshchaya Teoriya Obolochek i Yeye Prilozheniya v Tekhnike," Moscow, 1949.

[18]Vasiliev, V. V., *Mechanics of Composite Materials*, Taylor and Francis, Philadelphia, 1993.

[19]Arbocz, J., and Starnes, J. H., "A Hierarchical High/Fidelity Analysis Procedure for Buckling Critical Structures," *44th AIAA/ASME/ASCE/AHS Structures, Structural Dynamics, and Materials Conference*, Vol. 6, AIAA, Reston, VA, 2003, pp. 4100–4118.

[20]Hilburger, M. W., and Starnes, J. H., "Effects of Imperfections of the Buckling Response of Composite Shells," *Thin-Walled Structures*, Vol. 42, No. 3, 2004, pp. 369–397.

[21]Meyer-Piening, H.-R., Farshad, M., Geier, B., and Zimmermann, R., "Buckling Loads of CFRP Composite Cylinders Under Combined Axial and Torsion Loading—Experiments and Computations," *Composite Structures*, Vol. 53, No. 4, 2001, pp. 427–435.

[22]Stavsky, Y., and Hoff, N. J., "Mechanics of Composite Structures," *Composite Engineering Laminates*, edited by G. Dietz, MIT Press, Cambridge, MA, 1969, Chap. 1.

[23]Nemeth, M. P., "Nondimensional Parameters and Equations for Buckling of Anisotropic Shallow Shells," *Journal of Applied Mechanics*, Vol. 61, No. 3, 1994, pp. 664–669.

K. Shivakumar
Associate Editor